Impact of Timing Offset on Optical Spatial Pulse Position Modulation

Impact of Timing Offset on Optical Spatial Pulse Position Modulation

Hammed G. Olanrewaju, John Thompson, and Wasiu O. Popoola,

***Abstract*—This work investigates the impact of timing offset on the performance of an optical spatial modulation (OSM) technique termed spatial pulse position modulation (SPPM). SPPM combines optical spatial shift keying (OSSK) with pulse position modulation (PPM), exploiting the spatial domain to improve spectral the efficiency of PPM. In most works related to OSM, a perfect synchronization between the transmit and receive units is assumed. However, timing offset can result from clock jitter and variation in propagation delay of the transmit paths. Timing offset introduces intersymbol interference which can degrade system performance, hence the need to investigate its effect. Using the union bound technique, we derive the analytical upper bound on the symbol error rate (SER) of an SPPM-based optical wireless communication system that is impaired by timing offset. The analysis is validated via closely matching simulation results. Results show that error performance degrades as timing offset increases. For a small range of timing offset values, OSSK shows a better tolerance compared to SPPM.**

***Index Terms*—Optical wireless communication, multiple-input multiple-output (MIMO) systems, spatial modulation, synchronization, digital modulation.**

I. INTRODUCTION

Spatial modulation (SM) has been extensively studied as a promising multiple-input multiple-output (MIMO) technique which supports lower system complexity, reduced signal processing and improved energy-efficiency in wireless communication systems [1]–[5]. As a MIMO technique, SM employs multiple transmit elements, exploiting their spatial domain to convey all or some of the information bits of the transmitted symbol. SM schemes include space shift keying (SSK), [6] which encodes the information bits solely on the spatial index of the transmitters, and other variants which combine SSK with digital signal modulation such as pulse position modulation (PPM) [4], pulse amplitude modulation [7], quadrature amplitude modulation (QAM) [8] and orthogonal frequency division multiplexing (OFDM) [9], [10]. Spatial pulse position modulation (SPPM) [4] is an optical SM (OSM) scheme which combines optical SSK (OSSK) with PPM, exploiting the spatial domain to improve the spectral efficiency of PPM while still retaining its power efficiency.

Timing offsets in optical wireless MIMO systems can result from clock jitter, multipath propagation [12], [13], [19], the differences in propagation delay due to the physical separation of the transmitter and receiver arrays and receiver mobility. Such timing offsets cause the receiver to read a mixture of interfering signals at its sampling instant, and these interfering signals constitute intersymbol interference (ISI) which compromises accurate detection of the transmitted symbols.

As established in previous papers on SM, the performance of the SM technique is highly dependent on the dissimilarity of the channel gains of the transmit-receive paths [1], [7], [14]. To obtain dissimilar gains, physical spacing is provided between the units of the transmit and receive arrays. Due to this spacing, the transmit paths may experience different propagation characteristics such as path delay and this causes multiple timing offsets at the receiver, especially in high-speed communication. A similar variation in channel characteristics is expected if the receiver is moved from one point to another. Moreover, since additional information bits are encoded in the transmitted signal modulation, the sensitivity of the employed digital modulation to timing offset is also very relevant.

This paper analyses the impact of timing offset on the performance of optical SM using SPPM as a case study. A comprehensive investigation which provides a generalised framework for the analysis of the impact of synchronization error on different variants of OSM is detailed in our journal paper [15]. Specifically, using the union bound technique [16], we derive the analytical upper bound on the symbol error rate (SER) an SPPM-based optical wireless communication (OWC) system that is impaired by timing offset. Furthermore, simulations are performed to validate the analytical results, and the impact of channel gain on performance is demonstrated. Also, the performance comparison of the impact of timing offset on SPPM and OSSK is presented.

The rest of this paper is organized as follows: the system model for an SPPM-based OWC sytem is presented in Section II, and the analysis of the impact of timing offset on error performance is given in Section III. Section IV provides the analytical and simulation results of the performance evaluation and concluding remarks are given in Section V.

II. SYSTEM MODEL

Considering an OWC system with N_{t} Light emitting diodes (LEDs), using SPPM [4], only one LED is activated to send data signal during a given symbol duration, while the rest of the LEDs are idle. The activated LED transmits an $L-\mathrm{PPM}$ optical signal in each symbol duration, where L is the number of PPM time slots in a symbol duration. At the transmitter, a total of $M=\log_2(N_{\mathrm{t}}L)$ bits are transmitted per SPPM symbol. The first $\log_2(N_{\mathrm{t}})$ most significant bits constitute the spatial bits which determine the index (position) of the LED that will be activated, while the remaining $\log_2(L)$ bits constitute the signal bits which determine the pulse position of the transmitted PPM signal. For instance, in the SPPM encoding scheme illustrated in Fig. 1 for the case of $N_{\mathrm{t}}=4$, $L=4$ and

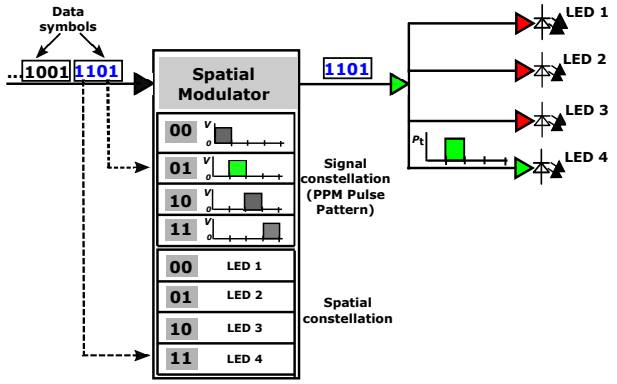

Fig. 1. Illustration of SPPM encoding using $N_{\rm t}=4$, $L=4$.

$M=4$ bits/symbol, the symbol '13' with binary representation '1101', is transmitted by activating 'LED 4' to transmit a pulse in the second slot. Each LED introduces a specific "channel signature" i.e., the channel path gain, that makes its emitted signal unique at the receiver compared to the same signal emitted by any other LED. The receiver exploits the uniqueness of the channel gains to retrieve the information bits. By using pilot symbols for channel estimation, the channel gains of the $N_{\rm t}$ LEDs are obtained at the receiver, and maximum likelihood (ML) detection is performed to estimate the transmitted symbol.

Without a loss of generality, we consider a single-receiver OWC system. Let $\mathcal{A}_{j,m}$ denote a single data symbol transmitted by activating the jth LED to transmit a pulse in slot m of the PPM signal, where $j \in [1, N_{\rm t}]$ and $m \in [1, L]$. Assuming no timing offset between the LED and the receiver, the received electrical signal in a single symbol duration T, is given by:

$$r(t) = s_{j,m}(t) + \eta(t), \quad 0 \le t \le T \tag{1}$$

where

$$s_{j,m}(t) = \begin{cases} h_j R P_{\rm t}; & \text{for } (m-1)T_{\rm c} \le t \le mT_{\rm c} \\ 0; & \text{elsewhere,} \end{cases} \tag{2}$$

R is the responsivity of the photodetector (PD), h_j is the channel gain between the jth LED and the receiver, $P_{\rm t}$ is the peak transmitted optical power, and the duration of each PPM time slot, $T_{\rm c} = T/L$. Considering a Silicon PIN PD with negligible dark current [13], [17], $\eta(t)$ is the sum of the ambient light shot noise and the thermal noise in the receiver, modelled as independent and identically distributed additive white Gaussian noise (AWGN) [11], [18].

The matched filter (MF) receiver architecture employs a rectangular pulse-shaping filter of amplitude $RP_{\rm t}$ and duration $T_{\rm c}$. The MF output in each time slot, obtained by sampling at the rate $1/T_{\rm c}$, is given by:

$$\begin{aligned} \mathbf{r} &= \mathbf{s}_{j,m} + \mathbf{n} \\ \{r_\ell\}_{\ell=1}^{L} &= \left\{ s_{j,m}^{\ell} + n_\ell \right\}_{\ell=1}^{L} \end{aligned} \tag{3}$$

where

$$s_{j,m}^{\ell} = \begin{cases} h_j E_{\rm s}; & \text{if } \ell = m \\ 0\,; & \text{otherwise,} \end{cases} \tag{4}$$

and $\{n_\ell\}_{\ell=1}^{L}$ are the L Gaussian noise samples at the output of the MF in each time slot, with variance $\sigma_n^2 = \frac{N_0}{2} E_{\rm s}$. The energy per symbol $E_{\rm s} = (RP_t)^2 T_{\rm c}$, and N_0 represents the noise power spectral density. Based on the ML detection criterion, the estimate of the transmitted symbol is obtained from the combination of the pulse position and the LED index which gives the minimum Euclidean distance from the received signal [4]. That is, the estimate of transmitted symbol, $\hat{\mathcal{A}}_{j,m}$, is obtained as:

$$\begin{aligned} \hat{\mathcal{A}}_{\hat{j},\hat{m}} = [\hat{j}, \hat{m}] &= \arg\max_{j,m} p\left(\mathbf{r}|\mathbf{s}_{j,m}\right) \\ &= \arg\min_{j,m} \left[D(\mathbf{r}, \mathbf{s}_{j,m}) \right]. \end{aligned} \tag{5}$$

The probability density function of $\mathbf{r}$ conditioned on $\mathbf{s}_{j,m}$ being transmitted is expressed as:

$$p\left(\mathbf{r}|\mathbf{s}_{j,m}\right) = \frac{1}{\left(2\pi\sigma_n^2\right)^{L/2}} \exp\left[-\frac{\left\|\mathbf{r} - \mathbf{s}_{j,m}\right\|^2}{2\sigma_n^2} \right], \tag{6}$$

and the Euclidean distance metric $D\left(\mathbf{r}, \mathbf{s}_{j,m}\right)$ is given as:

$$D\left(\mathbf{r}, \mathbf{s}_{j,m}\right) = \left\|\mathbf{r} - \mathbf{s}_{j,m}\right\|^2. \tag{7}$$

The notation $\|\cdot\|$ represents the Euclidean norm.

III. ERROR PERFORMANCE ANALYSIS

Considering a non-ideal system in which the received signal is impaired by timing offsets between the LEDs and the receiver, these timing offsets cause the receiver to read a mixture of interfering signals at its sampling instant, which may result in erroneous symbol detection. The theoretical analysis of such effects on the error performance of an SPPM-based OWC system is provided in this section.

Let $\mathcal{A}_{i,\mu}$ and $\mathcal{A}_{j,m}$, for $1 \le i, j \le N_{\rm t}$, $1 \le m, \mu \le L$, denote two consecutively transmitted symbols, such that $\mathcal{A}_{i,\mu}$ and $\mathcal{A}_{j,m}$ are transmitted in the previous and the current symbol duration respectively. Also, the timing offsets introduced into the signal received from each LED is denoted by $\mathbf{\Delta} = [\Delta_1, \ldots, \Delta_\kappa \ldots \Delta_{N_{\rm t}}]$. Positive timing offsets $(0 < \Delta_\kappa < T_{\rm c})$ are considered here, but the interpretation also holds for negative offsets. A positive offset implies that the received signal is lagging with respect to the receiver's clock. If symbol $\mathcal{A}_{j,m}$ is impaired by timing offset, then only a portion of its signal energy is included in the MF output for slot m, while the remaining signal energy is spilled over into the adjoining time slot, denoted by m^+.

By using (4), the portion of symbol $\mathcal{A}_{j,m}$'s energy that is captured in the MF output for slot m is obtained as $E_{\rm s} h_j (1 - \epsilon_j)$, while the the energy lost as spillover from slot m into the adjoining time slot m^+ is $E_{\rm s} h_j \epsilon_j$, where $\{\epsilon_\kappa\}_{\kappa=1}^{N_{\rm t}}$ represents the timing offsets normalised by the pulse (slot) duration $T_{\rm c}$, that is, $\epsilon_\kappa = \Delta_\kappa / T_{\rm c}$. Similarly, if symbol $\mathcal{A}_{i,\mu}$ is impaired by timing offset, then the lost (spillover) energy from slot μ into the adjoining time slot μ^+ is $E_{\rm s} h_i \epsilon_i$.

The effect of the ISI which results from the energy spillovers described above, depends on the pulse position of both symbols $\mathcal{A}_{i,\mu}$ and $\mathcal{A}_{j,m}$, i.e., the indices of time slots, m and μ, $1 \leq m, \mu \leq L$. In the following derivations, all the possible pulse position combinations are considered.

A transmitted symbol is correctly decoded if both the pulse position and the LED index are correctly decoded. Thus, the probability of symbol error is expressed as:

$$P_{\mathrm{e,sym}} = 1 - \left(P_{\mathrm{c,tx}} \times P_{\mathrm{c,ppm}}\right), \tag{8}$$

where $P_{\mathrm{c,ppm}} = p(\hat{m} = m)$, is the probability of a correctly decoded pulse position, and $P_{\mathrm{c,tx}} = p(\hat{j} = j | \hat{m} = m)$, is the probability of correctly decoding the index of the activated LED, given that the pulse position has been correctly decoded. The expressions for $P_{\mathrm{c,tx}}$ and $P_{\mathrm{c,ppm}}$ are derived as follows.

A. Impact of timing offset on the detection of activated LED

For symbol $\mathcal{A}_{j,m}$, the pairwise error probability (PEP) that the receiver decides in favour of LED k instead of j, is:

$$\mathrm{PEP}_m^{j \to k} = \mathbb{P}[D(\overline{\mathbf{r}}, \mathbf{s}_{j,m}) > D(\overline{\mathbf{r}}, \mathbf{s}_{k,m})] \tag{9}$$

where $\overline{\mathbf{r}} = \{\overline{r}_\ell\}_{\ell=1}^{L}$ is the sampled MF output which has been impaired by ISI due to timing offset. The notation $\mathbb{P}[\cdot]$ represents the probability of occurrence. Using equations (4) and (7) in (9), we obtain [4]:

$$\mathrm{PEP}_m^{j \to k} = \mathbb{P}\left[(\overline{r}_m - h_j E_{\mathrm{s}})^2 > (\overline{r}_m - h_k E_{\mathrm{s}})^2\right]. \tag{10}$$

As mentioned earlier, the value of $\overline{r}_m$ in (10) depends on the position of the transmitted pulses in symbols $\mathcal{A}_{i,\mu}$ and $\mathcal{A}_{j,m}$. For two symbols with L-PPM pulse pattern, there are L^2 possible pulse position combinations which are grouped under two cases as follows.

*1) **Case I**:* If $1 \leq \mu < L$ or $1 < m \leq L$, then, there is no spillover energy from $\mathcal{A}_{i,\mu}$ into the pulse position (slot m) of $\mathcal{A}_{j,m}$. Therefore, $\overline{r}_m = E_{\mathrm{s}} h_j (1 - \epsilon_j) + n_m$, and the PEP for this case is obtained from (6) and (10) as:

$$\begin{aligned}
\mathrm{PEP}_m^{\mathrm{I},j \to k} &= \mathbb{P}[2 n_m (h_k - h_j) > E_{\mathrm{s}} \Omega_{\mathrm{I}}] \\
&= \int_{\frac{E_{\mathrm{s}} \Omega_{\mathrm{I}}}{2|h_k - h_j|}}^{\infty} \frac{1}{\sqrt{2\pi\sigma_n^2}} \exp\left(-\frac{x^2}{2\sigma_n^2}\right) \\
&= Q\left(\frac{\Omega_{\mathrm{I}}}{|h_k - h_j|} \sqrt{\frac{\gamma_{\mathrm{s}}}{2}}\right)
\end{aligned} \tag{11}$$

where

$$\Omega_{\mathrm{I}} = h_j^2 (1 - 2\epsilon_j) + 2 h_j h_k (\epsilon_j - 1) + h_k^2, \tag{12}$$

$h_k \neq h_j$, $Q(\cdot)$ denotes the Q-function and the symbol signal-to-noise ratio (SNR) is $\gamma_{\mathrm{s}} = E_{\mathrm{s}}/N_0$. Out of the L^2 possible combinations, the probability of occurrence for this case is:

$$\Phi_{\mathrm{I}} = \mathbb{P}\left[1 \leq \mu < L\right] \times \mathbb{P}\left[1 < m \leq L\right] = (L^2 - 1)/L^2. \tag{13}$$

In the diagrammatic illustration in Fig. 2, Cases A, B, D and E are instances of this Case I.

*2) **Case II**:* For this case, $\mu = L$ and $m = 1$. Thus, any spillover energy from $\mathcal{A}_{i,\mu}$ is contributed into slot m of $\mathcal{A}_{j,m}$. Hence, $\overline{r}_m = E_{\mathrm{s}}(h_j(1 - \epsilon_j) + h_i \epsilon_i) + n_m$. Similar to Case I above, the PEP for this case is obtained as:

$$\mathrm{PEP}_m^{\mathrm{II},j \to k} = \frac{1}{N_{\mathrm{t}}} \sum_{i=1}^{N_{\mathrm{t}}} Q\left(\frac{\Omega_{\mathrm{II}}}{|h_k - h_j|} \sqrt{\frac{\gamma_{\mathrm{s}}}{2}}\right), \tag{14}$$

where

$$\Omega_{\mathrm{II}} = h_j^2 (1 - 2\epsilon_j) + 2 h_j h_k (\epsilon_j - 1) + h_k^2 + 2 h_i \epsilon_i (h_j - h_k),$$

and the probability of occurrence is given by:

$$\Phi_{\mathrm{II}} = \mathbb{P}\left[\mu = L\right] \times \mathbb{P}\left[m = 1\right] = 1/L^2. \tag{15}$$

In the diagrammatic illustration in Fig. 2, Case C represents an instance of this Case II.

Note that the symbol $\mathcal{A}_{i,\mu}$ can be transmitted by activating any of the equiprobable N_{t} LEDs. Hence, $\mathrm{PEP}_m^{\mathrm{II},j \to k}$ is obtained by taking the average over N_{t} LEDs, as shown in (14). By combining (11) and (14), the PEP of decoding the activated LED is given by:

$$\mathrm{PEP}_m^{j \to k} = (\Phi_{\mathrm{I}} \times \mathrm{PEP}_m^{\mathrm{I},j \to k}) + (\Phi_{\mathrm{II}} \times \mathrm{PEP}_m^{\mathrm{II},j \to k}). \tag{16}$$

Using the union bound technique [16], for N_{t} LEDs, the probability of correctly decoding the activated LED, conditioned on a correctly decoded pulse position, is given by (17) (at the top of the next page).

B. Impact of timing offset on the detection of pulse position

For the transmitted symbol $\mathcal{A}_{j,m}$, the PEP that the receiver decides in favour of slot q instead of slot m is expressed as:

$$\begin{aligned}
\mathrm{PEP}_{m \to q}^{j} &= \mathbb{P}[D(\overline{\mathbf{r}}, \mathbf{s}_{j,m}) > D(\overline{\mathbf{r}}, \mathbf{s}_{j,q})] \\
&= \mathbb{P}\left[(\overline{r}_m - s_{j,m})^2 + \overline{r}_q^2 > \overline{r}_m^2 + (\overline{r}_q - s_{j,q})^2\right]
\end{aligned} \tag{18}$$

As in Section III-A, the values of $\overline{r}_m$ and $\overline{r}_q$, and hence $\mathrm{PEP}_{m \to q}^{j}$, depend on the index of slot m and q in the PPM signal of symbol $\mathcal{A}_{j,m}$, and on the index of slot μ in the PPM signal of symbol $\mathcal{A}_{i,\mu}$. All the possible pulse position combinations are grouped into 5 different cases, and the diagrammatic illustration of these five cases for a 4-PPM pulse pattern is shown in Fig. 2. A summary of the parameters and the expressions for $\overline{r}_m$ and $\overline{r}_q$ for each of the 5 cases is provided in Table I.

*1) **Case A**:* For this case, $1 \leq \mu < L$ and $1 \leq m < L$. Hence, no spillover energy from $\mathcal{A}_{i,\mu}$ is contributed to the MF output in the first slot of $\mathcal{A}_{j,m}$. Using Table I, the probability of error in decoding the pulse position in this case is:

$$\mathcal{P}_{\mathrm{A}} = \Phi_{\mathrm{A}} \times \left(\mathrm{PEP}_{m \to m^+}^{j} + (L - 2)\ \mathrm{PEP}_{m \to q}^{j}\right), \tag{19}$$

where Φ_{A} is the probability of occurrence for this case, $\mathrm{PEP}_{m \to m+}^{j}$ is the PEP between slot m and the adjacent slot m^+, while $\mathrm{PEP}_{m \to q}^{j}$, for $\{1 \leq q \leq L,\ q \neq m, q \neq m^+\}$, is the PEP between slot m and any of the other $(L - 2)$ empty slots in $\mathcal{A}_{j,m}$.

*2) **Case B**:* As in case A above, $1 \leq \mu < L$. But, for symbol $\mathcal{A}_{j,m}$, $m = L$. Hence, any spillover energy from $\mathcal{A}_{j,m}$ is

$$P_{\mathrm{c,tx}} \;\leq\; 1-\frac{1}{N_{\mathrm{t}}}\sum_{j=1}^{N_{\mathrm{t}}}\sum_{\substack{k=1\\k\neq j}}^{N_{\mathrm{t}}}\mathrm{PEP}_{m}^{j\to k} \;=\; 1-\frac{1}{N_{\mathrm{t}}L^2}\sum_{j=1}^{N_{\mathrm{t}}}\sum_{\substack{k=1\\k\neq j}}^{N_{\mathrm{t}}}\Big((L^2-1)\mathrm{PEP}_{m}^{\mathrm{I},j\to k} \;+\; \mathrm{PEP}_{m}^{\mathrm{II},j\to k}\Big). \tag{17}$$

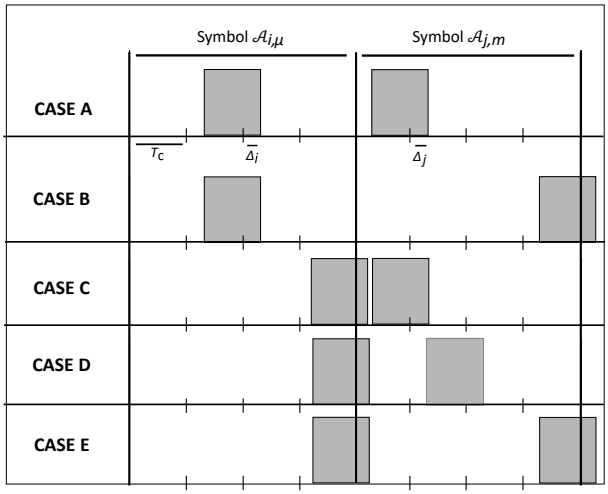

Fig. 2. Illustration of the impact of timing offset with different pulse position combinations for symbols $\mathcal{A}_{i,\mu}$ and $\mathcal{A}_{j,m}$ in an SPPM scheme with 4 time slots.

contributed to the first slot of the next symbol. The probability of error in decoding the pulse position in this case is:

$$\mathcal{P}_{\mathrm{B}} = \Phi_{\mathrm{B}} \times (L-1)\ \mathrm{PEP}_{m\to q}^{j}, \tag{20}$$

where $\mathrm{PEP}_{m\to q}^{j}$ for $1 \leq q \leq (L-1)$, is the PEP between slot m and any of the other $(L-1)$ empty slots.

*3) **Case C**:* In this case, $\mu = L$ and $m = 1$. Hence, any spillover energy from $\mathcal{A}_{i,\mu}$, is contributed to the MF output in slot m of symbol $\mathcal{A}_{j,m}$. The probability of error in decoding the pulse position is:

$$\mathcal{P}_{\mathrm{C}} = \frac{\Phi_{\mathrm{C}}}{N_{\mathrm{t}}}\sum_{i=1}^{N_{\mathrm{t}}}\Big(\mathrm{PEP}_{m\to m^{+}}^{j} \;+\; (L-2)\ \mathrm{PEP}_{m\to q}^{j}\Big), \tag{21}$$

where $\mathrm{PEP}_{m\to m+}^{j}$ is the PEP between slot m and the next slot m^{+}, while $\mathrm{PEP}_{m\to q}^{j}$, for $3 \leq q \leq L$, is the PEP between slot m and any of the other $(L-2)$ empty slots.

*4) **Case D**:* For this case, $\mu = L$, $1 < m < L$, and the probability of error in decoding the pulse position in this case is given by:

$$\mathcal{P}_{\mathrm{D}} \;=\; \frac{\Phi_{\mathrm{D}}}{N_{\mathrm{t}}}\sum_{i=1}^{N_{\mathrm{t}}}\big(\mathrm{PEP}_{m\to 1}^{j} + \mathrm{PEP}_{m\to m^{+}}^{j} + (L-3)\mathrm{PEP}_{m\to q}^{j}\big), \tag{22}$$

where $\mathrm{PEP}_{m\to 1}^{j}$ is the PEP between slot m and the first slot, $\mathrm{PEP}_{m\to m+}^{j}$ is the PEP between slot m and the adjacent slot m^{+}, while $\mathrm{PEP}_{m\to q}^{j}$ is the PEP between slot m and any of the other $(L-3)$ empty slots.

*5) **Case E**:* In this scenario, $\mu = L$, $m = L$, and the probability of error in decoding the pulse position is:

$$\mathcal{P}_{\mathrm{E}} = \frac{\Phi_{\mathrm{E}}}{N_{\mathrm{t}}}\sum_{i=1}^{N_{\mathrm{t}}}\Big(\mathrm{PEP}_{m\to 1}^{j} + (L-2)\mathrm{PEP}_{m\to q}^{j}\Big), \tag{23}$$

where $\mathrm{PEP}_{m\to 1}^{j}$ is the PEP between slot m and the first slot, and $\mathrm{PEP}_{m\to q}^{j}$ for $1 < q < L$, is the PEP between slot m and any of the other $(L-2)$ empty slots.

The PEP terms in (19), (20), (21), (22) and (23), are given in Table I. They are obtained by using the corresponding expressions for $\overline{r}_m$ and $\overline{r}_q$ provided in Table I. Thus, for N_{t} LEDs, the probability of correctly decoding the pulse position of the transmitted data symbol is given by:

$$P_{\mathrm{c,ppm}} = 1 - \frac{1}{N_{\mathrm{t}}}\sum_{j=1}^{N_{\mathrm{t}}}\left(\mathcal{P}_{\mathrm{A}} + \mathcal{P}_{\mathrm{B}} + \mathcal{P}_{\mathrm{C}} + \mathcal{P}_{\mathrm{D}} + \mathcal{P}_{\mathrm{E}}\right). \tag{24}$$

Combining (17) and (24), the average symbol error probability for an SPPM scheme that is impaired by timing offsets, is given by (25). By setting the timing offsets to zero, i.e., $\{\epsilon_\kappa\}_{\kappa=1}^{N_{\mathrm{t}}} = 0$, the derived expression in (25) reduces to the standard SER expression for SPPM scheme without timing errors [4, Eq. (23)]. Also, the analysis of the impact of timing offset on an OSSK scheme can be done by following the procedure presented above for SPPM. The SER of an OSSK scheme that is impaired by timing offset is obtained by setting $L = 1$ in (25).

IV. RESULTS AND DISCUSSION

In this section, we present the analytical and simulation results of the impact of timing offset on SPPM scheme. The achieved SER is plotted against the SNR per bit γ_{b}. The channel response is obtained from the simulation of indoor OWC channel based on geometrical modelling of a $(5 \times 5 \times 3)$m indoor reflective environments and ray-tracing/multiple-bounce iterative technique presented in [19]. The transmitter coordinates are (1.25,1.25,3), (1.25,3.75,3), (3.75,1.25,3) and (3.75,3.75,3), while the receiver is positioned at (1.0,2.0,0). Details of other simulation parameters can be found in [19]. The normalized channel gain values for 4 LEDs are $\{h_j\}_{j=1}^{N_{\mathrm{t}}} = [1, 0.601, 0.332, 0.1334]$.

Considering the worst-case scenario where timing offset exists in the signal received from all the LEDs, Fig. 3 depicts the error performance plots for different timing offsets, using $N_{\mathrm{t}} = 2, L = 2$. The plots clearly show that the analytical upper bound in (25) matches the simulation result very closely. The results also show that due to the ISI caused by timing offset, the performance of the system is degraded. For example, at SER = 10^{-5}, compared to the zero-offset case ($\epsilon = 0$),

$$P_{\mathrm{e,sym}}^{\mathrm{SPPM}} \leq 1 - \left(1 - \frac{1}{N_{\mathrm{t}}} \sum_{j=1}^{N_{\mathrm{t}}} \sum_{\substack{k=1 \\ k \neq j}}^{N_{\mathrm{t}}} \mathrm{PEP}_m^{j \to k}\right) \left(1 - \frac{1}{N_{\mathrm{t}}} \sum_{j=1}^{N_{\mathrm{t}}} (\mathcal{P}_{\mathrm{A}} + \mathcal{P}_{\mathrm{B}} + \mathcal{P}_{\mathrm{C}} + \mathcal{P}_{\mathrm{D}} + \mathcal{P}_{\mathrm{E}})\right). \tag{25}$$

TABLE I
SUMMARY OF THE PARAMETERS AND EXPRESSIONS FOR DIFFERENT PULSE POSITION COMBINATIONS IN AN SPPM SCHEME IMPAIRED BY TIMING OFFSET.

CASE	μ	m	$\overline{r}_m$	q	$\overline{r}_q$	$\mathrm{PEP}_{m\to q}^{j}$	Φ
A	$1 \leq \mu < L$	$1 \leq m < L$	$h_j E_{\mathrm{s}}(1-\epsilon_j) + n_m$	m^+	$h_j E_{\mathrm{s}} \epsilon_j + n_q$	$Q\big(h_j(1-2\epsilon_j)\sqrt{\gamma_{\mathrm{s}}}\big)$	$\left(\frac{L-1}{L}\right)^2$
				$1 \leq q \leq L$, $q \neq m, q \neq m^+$	n_q	$Q\big(h_j(1-\epsilon_j)\sqrt{\gamma_{\mathrm{s}}}\big)$	
B		L	$h_j E_{\mathrm{s}}(1-\epsilon_j) + n_m$	$1 \leq q \leq (L-1)$	n_q	$Q\big(h_j(1-\epsilon_j)\sqrt{\gamma_{\mathrm{s}}}\big)$	$\frac{L-1}{L^2}$
C	L	1	$h_j E_{\mathrm{s}}(1-\epsilon_j) + h_i E_{\mathrm{s}} \epsilon_i + n_m$	m^+	$h_j E_{\mathrm{s}} \epsilon_j + n_q$	$Q\Big(\big(h_j(1-2\epsilon_j) + h_i\epsilon_i\big)\sqrt{\gamma_{\mathrm{s}}}\Big)$	$\frac{1}{L^2}$
				$3 \leq q \leq L$	n_q	$Q\Big(\big(h_j(1-\epsilon_j) - h_i\epsilon_i\big)\sqrt{\gamma_{\mathrm{s}}}\Big)$	
D		$1 < m < L$	$h_j E_{\mathrm{s}}(1-\epsilon_j) + n_m$	1	$h_i E_{\mathrm{s}} \epsilon_i + n_q$	$Q\Big(\big(h_j(1-\epsilon_j) + h_i\epsilon_i\big)\sqrt{\gamma_{\mathrm{s}}}\Big)$	$\frac{(L-2)}{L^2}$
				m^+	$h_j E_{\mathrm{s}} \epsilon_j + n_q$	$Q\Big(\big(h_j(1-\epsilon_j) + h_i\epsilon_i\big)\sqrt{\gamma_{\mathrm{s}}}\Big)$	
				$2 \leq q \leq L$, $q \neq m, q \neq m^+$	n_q	$Q\Big(\big(h_j(1-2\epsilon_j) + h_i\epsilon_i\big)\sqrt{\gamma_{\mathrm{s}}}\Big)$	
E		L	$h_j E_{\mathrm{s}}(1-\epsilon_j) + n_m$	1	$h_i E_{\mathrm{s}} \epsilon_i + n_q$	$Q\Big(\big(h_j(1-\epsilon_j) - h_i\epsilon_i\big)\sqrt{\gamma_{\mathrm{s}}}\Big)$	$\frac{1}{L^2}$
				$1 < q < L$	n_q	$Q\big(h_j(1-\epsilon_j)\sqrt{\gamma_{\mathrm{s}}}\big)$	

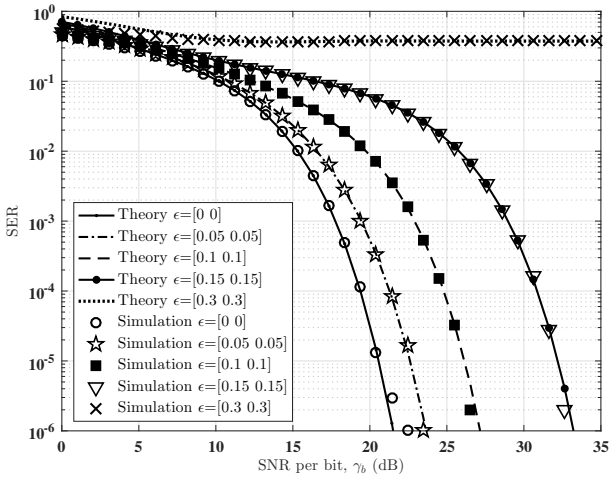

Fig. 3. Error performance of SPPM. $N_{\mathrm{t}} = 2$, $L = 2$. Channel gains: $[h_1, h_2] = [1, 0.601]$. Normalised offset: $\epsilon_1 = \epsilon_2 = \epsilon$, $\epsilon = \Delta/T_{\mathrm{c}}$.

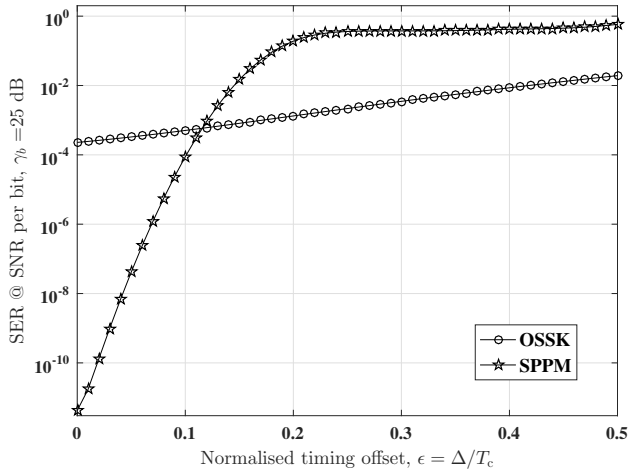

Fig. 4. Comparison of the effect of timing offset on OSSK and SPPM, $N_{\mathrm{t}} = 2$, $L = 2$. Channel gains: $[h_1, h_2] = [1, 0.601]$.

a timing offset of 10% of the pulse (slot) duration results in SNR penalty of about 5 dB.

In Fig. 4 the effect of timing offset on an SPPM scheme is compared with that of an OSSK scheme. For a fair comparison, both schemes are implemented with equal average energy per symbol, and the timing offset is normalised to the slot duration. Using $N_{\mathrm{t}} = 2, L = 2$, the achieved SER at $\gamma_{\mathrm{b}} = 25$ dB, for different timing offsets is shown in Fig. 4. The specified timing offsets are assigned to both LEDs concurrently. It can be observed in Fig. 4 that the effect of timing offset is more significant in SPPM compared to OSSK, as indicated by the slope of the plot for each scheme. The results show that as the offset increases, the SER of SPPM increases at a faster rate compared to that of OSSK. For instance, compared to the zero-offset case ($\epsilon = 0$), a timing offset of 10% of the slot duration, increases the SER from 10^{-12} to 10^{-4} in SPPM, while the same amount of timing offset increases the SER by only a factor of 3 in OSSK. Though SPPM still achieved a better SER compared to OSSK for $0 \leq \epsilon < 0.12$), the energy efficiency benefit harnessed from PPM is however rapidly lost to timing offset due to the sensitivity of PPM to synchronization error [20], [21].

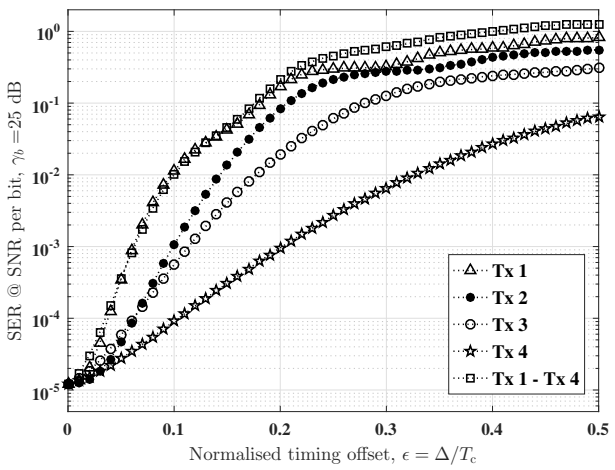

Fig. 5. Impact of channel gain values (transmitter location) on the error performance of SPPM with timing offsets. $N_t = 4$, $L = 2$, Tx denotes transmit units, channel gains: $\{h_i\}_{i=1}^{Nt} = [1, 0.601, 0.332, 0.1334]$.

In Fig. 5, we illustrate the impact of channel gain values (LED location) on the system performance. Using four LEDs, first, timing offset is introduced in only one of the LEDs at a time. Then, we set equal timing offset in all the four LEDs concurrently. In all the cases, we estimate the achieved SER at $\gamma_b = 25$ dB. Figure 5 shows that the lower the channel gain of the transmit path in which timing error occurs, the lesser the impact of the timing error on the system performance. For a timing offset of 10% of the pulse duration, the achieved SER is 6×10^{-4} if the offset occurs in transmitter 3 ($h_3 = 0.332$) and SER $= 10^{-4}$ if the offset occurs in transmitter 4 ($h_4 = 0.1334$). This result highlights the dependence of the performance of SM technique on the channel gain values of the transmitters.

V. Conclusion

The impact of timing offset between transmit and receive array on optical SPPM has been investigated in this paper. For an SPPM-based OWC system that is impaired by timing offset, the theoretical expression for the SER is derived and validated by tightly-matched simulation results. The results provide insight into how synchronization error due to timing offset affects the performance of spatial modulation techniques. The performance of the system degrades with increasing timing offsets. A comparison of the effect of timing offset on the error performance highlights the tolerance of OSSK to small range of timing offset values compared to SPPM, though the former offers the lower throughput. A 10% offset results in an increase in SER by a factor of 3 in OSSK and a factor of 10^8 in SPPM. These results show that accurate synchronization is necessary for SM techniques, especially when digital signal modulation is employed to convey additional information bits.

References

[1] M. Di Renzo, H. Haas, and P. M. Grant, "Spatial modulation for multiple-antenna wireless systems: a survey," *IEEE Communications Magazine*, vol. 49, no. 12, pp. 182–191, 2011.

[2] P. Yang, M. Di Renzo, Y. Xiao, S. Li, and L. Hanzo, "Design guidelines for spatial modulation," *IEEE Communications Surveys & Tutorials*, vol. 17, no. 1, pp. 6–26, 2015.

[3] R. Mesleh, H. Elgala, and H. Haas, "Optical spatial modulation," *Journal of Optical Communications and Networking*, vol. 3, no. 3, pp. 234–244, 2011.

[4] W. O. Popoola, E. Poves, and H. Haas, "Spatial pulse position modulation for optical communications," *Journal of Lightwave Technology*, vol. 30, no. 18, pp. 2948–2954, 2012.

[5] ——, "Error performance of generalised space shift keying for indoor visible light communications," *IEEE Transactions on Communications*, vol. 61, no. 5, pp. 1968–1976, 2013.

[6] J. Jeganathan, A. Ghrayeb, L. Szczecinski, and A. Ceron, "Space shift keying modulation for MIMO channels," *IEEE Transactions on Wireless Communications*, vol. 8, no. 7, pp. 3692–3703, 2009.

[7] T. Fath and H. Haas, "Performance comparison of MIMO techniques for optical wireless communications in indoor environments," *IEEE Transactions on Communications*, vol. 61, no. 2, pp. 733–742, 2013.

[8] P. Yang, Y. Xiao, Y. L. Guan, K. Hari, A. Chockalingam, S. Sugiura, H. Haas, M. Di Renzo, C. Masouros, Z. Liu *et al.*, "Single-carrier SM-MIMO: A promising design for broadband large-scale antenna systems," *IEEE Communications Surveys & Tutorials*, vol. 18, no. 3, pp. 1687–1716, 2016.

[9] R. Y. Mesleh, H. Haas, S. Sinanovic, C. W. Ahn, and S. Yun, "Spatial modulation," *IEEE Transactions on Vehicular Technology*, vol. 57, no. 4, pp. 2228–2241, 2008.

[10] X. Zhang, S. Dimitrov, S. Sinanovic, and H. Haas, "Optimal power allocation in spatial modulation OFDM for visible light communications," in *2012 IEEE 75th Vehicular Technology Conference (VTC Spring)*. IEEE, 2012, pp. 1–5.

[11] J. M. Kahn and J. R. Barry, "Wireless infrared communications," *Proceedings of the IEEE*, vol. 85, no. 2, pp. 265–298, 1997.

[12] K. Lee, H. Park, and J. R. Barry, "Indoor Channel Characteristics for Visible Light Communications," *IEEE Communications Letters*, vol. 15, no. 2, pp. 217–219, 2011.

[13] Z. Ghassemlooy, W. Popoola, and S. Rajbhandari, *Optical wireless communications: system and channel modelling with Matlab®*. CRC Press, 2012.

[14] W. O. Popoola and H. Haas, "Demonstration of the merit and limitation of generalised space shift keying for indoor visible light communications," *Journal of Lightwave Technology*, vol. 32, no. 10, pp. 1960–1965, 2014.

[15] H. G. Olanrewaju and W. O. Popoola, "Effect of synchronization error on optical spatial modulation," *IEEE Transactions on Communications*, vol. 65, no. 12, pp. 5362–5374, 2017.

[16] J. Proakis and M. Salehi, *Digital communications*, 5th ed. McGraw-Hill, 2008.

[17] F. Xu, M.-A. Khalighi, and S. Bourennane, "Impact of different noise sources on the performance of PIN-and APD-based FSO receivers," in *Proceedings of the 2011, 11th International Conference on Telecommunications (ConTEL)*. IEEE, 2011, pp. 211–218.

[18] M. A. Khalighi and M. Uysal, "Survey on free space optical communication: A communication theory perspective," *IEEE Communications Surveys & Tutorials*, vol. 16, no. 4, pp. 2231–2258, 2014.

[19] J. R. Barry, J. M. Kahn, W. J. Krause, E. A. Lee, and D. G. Messerschmitt, "Simulation of multipath impulse response for indoor wireless optical channels," *IEEE journal on selected areas in communications*, vol. 11, no. 3, pp. 367–379, 1993.

[20] R. M. Gagliardi and S. Karp, *Optical communications*, 2nd ed. Wiley, 1995.

[21] S. Arnon, "The effect of clock jitter in visible light communication applications," *Journal of Lightwave Technology*, vol. 30, no. 21, pp. 3434–3439, 2012.